GLIA

WILEY

RESEARCH ARTICLE

Lithium inhibits tryptophan catabolism via the inflammation-induced kynurenine pathway in human microglia

Ria Göttert[1,2] 🔵 | Pawel Fidzinski[1,3,4] | Larissa Kraus[1,3] | Ulf Christoph Schneider[5] | Martin Holtkamp[1,3] | Matthias Endres[1,2,4,6,7] | Karen Gertz[1,2] | Golo Kronenberg[1,2,8,9,10]

[1]Charité-Universitätsmedizin Berlin, Corporate Member of Freie Universität Berlin, Humboldt-Universität zu Berlin, and Berlin Institute of Health, Klinik für Neurologie und Abteilung für Experimentelle Neurologie, Berlin, Germany

[2]Center for Stroke Research Berlin (CSB), Berlin, Germany

[3]Epilepsy-Center Berlin-Brandenburg, Berlin, Germany

[4]NeuroCure Cluster of Excellence, Berlin, Germany

[5]Charité-Universitätsmedizin Berlin, Corporate Member of Freie Universität Berlin, Humboldt-Universität zu Berlin, and Berlin Institute of Health, Klinik für Neurochirurgie, Berlin, Germany

[6]German Center for Neurodegenerative Diseases (DZNE), Partner Site Berlin, Berlin, Germany

[7]German Centre for Cardiovascular Research (DZHK), Partner Site Berlin, Berlin, Germany

[8]College of Life Sciences, University of Leicester, Leicester, UK

[9]Leicestershire Partnership National Health Service Trust, Leicester, UK

[10]Klinik für Psychiatrie, Psychotherapie und Psychosomatik, Psychiatrische Universitätsklinik Zürich, Zürich, Switzerland

Correspondence
Golo Kronenberg, Farm Lodge, Farm Drive, Leicester LE3 9Q4, UK.
Email: gdk7@leicester.ac.uk
Karen Gertz, Charitéplatz 1, 10117 Berlin, Germany.
Email: karen.gertz@charite.de

Abstract

Despite its decades' long therapeutic use in psychiatry, the biological mechanisms underlying lithium's mood-stabilizing effects have remained largely elusive. Here, we investigated the effect of lithium on tryptophan breakdown via the kynurenine pathway using immortalized human microglia cells, primary human microglia isolated from surgical specimens, and microglia-like cells differentiated from human induced pluripotent stem cells. Interferon (IFN)-γ, but not lipopolysaccharide, was able to activate immortalized human microglia, inducing a robust increase in indoleamine-2,3-dioxygenase (*IDO1*) mRNA transcription, IDO1 protein expression, and activity. Further, chromatin immunoprecipitation verified enriched binding of both STAT1 and STAT3 to the *IDO1* promoter. Lithium counteracted these effects, increasing inhibitory $GSK3\beta^{S9}$ phosphorylation and reducing $STAT1^{S727}$ and $STAT3^{Y705}$ phosphorylation levels in IFN-γ treated cells. Studies in primary human microglia and hiPSC-derived microglia confirmed the anti-inflammatory effects of lithium, highlighting that IDO activity is reduced by GSK3 inhibitor SB-216763 and STAT inhibitor

Karen Gertz and Golo Kronenberg contributed equally to this work.

nifuroxazide via downregulation of P-STAT1^{S727} and P-STAT3^{Y705}. Primary human microglia differed from immortalized human microglia and hiPSC derived microglia-like cells in their strong sensitivity to LPS, resulting in robust upregulation of IDO1 and anti-inflammatory cytokine IL-10. While lithium again decreased IDO1 activity in primary cells, it further increased release of IL-10 in response to LPS. Taken together, our study demonstrates that lithium inhibits the inflammatory kynurenine pathway in the microglia compartment of the human brain.

KEYWORDS
depression, kynurenine, lithium, microglia, tryptophan

1 | INTRODUCTION

The monovalent cation lithium has been in medical use for decades. Lithium remains a mainstay in the treatment and prophylaxis of bipolar disorder (Geddes et al., 2004; Malhi et al., 2017). Lithium is also effective in the prophylaxis of severe unipolar major depression (Tiihonen, 2017), and adjunctive lithium constitutes a promising therapeutic approach for patients who do not respond adequately to antidepressants (e.g., Bauer et al., 2010). Moreover, numerous reports have found that lithium exerts anti-suicidal effects in patients with mood disorders (reviewed in Smith & Cipriani, 2017).

Immunological mechanisms and, in particular, microglia activation, seem to play an important role in the etiopathogenesis of affective disorders in human patients and social-defeat induced behavioral changes in rodents (e.g., Jeon & Kim, 2016; Kopschina Feltes et al., 2017; McKim et al., 2018; Nie et al., 2018; Torres-Platas et al., 2014; Yirmiya et al., 2015). Upregulation of indoleamine-2,3-dioxygenase (IDO1), the rate-limiting enzyme converting tryptophan into kynurenine in activated microglia, may underlie reduced availability of serotonin in neuroinflammation. Anti-inflammatory effects of lithium have been reported by a number of recent studies (e.g., Ajmone-Cat et al., 2016; Cao et al., 2017; Dong et al., 2014). Moreover, numerous case reports have documented an increased risk of serotonin syndrome precipitated by co-prescription of lithium with antidepressants (e.g., Adan-Manes et al., 2006; Prakash et al., 2017; Sobanski et al., 1997). A study in rats treated with chronic lithium found increased levels of tryptophan alongside increased concentrations of serotonin metabolite 5-hydroxyindole acetic acid (5-HIAA) in brain (Perez-Cruet et al., 1971). Notwithstanding these observations, the effect of lithium on kynurenine pathway activity has not been investigated prior to this study. Using immortalized microglia, primary adult human microglia cultured from surgical specimens, and human iPSC-derived microglia-like cells, we herein confirmed the hypothesis that lithium decreases IDO1 activity in activated microglia and studied the underlying intracellular signaling pathways.

2 | MATERIALS AND METHODS

A key resources table is provided in Table S1.

2.1 | Human brain specimens

Human brain cortical biopsy material was obtained, after prior written informed consent, from patients undergoing surgery for medication-resistant epilepsy. All procedures were approved by the local ethics committee of the Charité-Universitätsmedizin Berlin (EA2/111/14) and performed in accordance with the Declaration of Helsinki.

All surgical specimens represent temporal resections from epileptic patients. Neuropathologic evaluation yielded no evidence of neoplastic tissue. The maximum degree of hippocampal sclerosis according to the International League Against Epilepsy (ILAE) classification (Blumcke et al., 2013) was 2. The age and sex of the patients included in this study are given in Figure S3f.

2.2 | Immortalized human microglia

Immortalized human microglia (HM-IM; Innoprot) were cultivated on collagen A coated plasticware in microglia medium (Innoprot) for up to eight passages. Cells were seeded and cultured at a density of 3×10^4 cells/cm^2 until they reached a confluence of 90%. To stop proliferation, cells were incubated for an additional 24 h in RPMI 1640 medium (Biochrom, Merck) lacking fetal calf serum before further experimentation. The measurement times were chosen based on pilot tests studying a range of lithium concentrations (Figure S1a–c) and the time course of IDO1 gene and protein expression after stimulation with IFN-γ (Figure S1d, f).

2.3 | Human induced pluripotent stem cells

Human induced pluripotent stem cells (hiPSC) lines (BIHi005-A, BIHi004-A, and BIHi001-A, see hPSCreg database for details https://hpscreg.eu) were provided by the Berlin Institute of Health (BIH) stem cell core facility.

HiPSCs were maintained in six-well plates (Corning) in feeder-free conditions using growth factor-reduced Geltrex (Thermo Fisher Scientific) coated culture dishes in complete TeSR-E8 medium (Stem Cell Technologies) and cultured in a humidified incubator (5% CO_2, 37°C). HiPSCs were fed daily with fresh media and passaged every 7–8 days.

2.4 | Reagents

Plasticware was coated with poly-L-lysin (diluted 1:20 in distilled water; Biochrom, Merck) or collagen A (0.5 mg/ml Biochrom, Merck) overnight at 4°C followed by washes with 1xDPBS (Gibco™, Thermo Fisher Scientific). Cells were activated with LPS (1 μg/ml; Sigma-Aldrich) or human IFN-γ (200 ng/ml; Peprotech). Lithium chloride (10 mM; Sigma-Aldrich), SB-216763 (10 μM; AdipoGen), and nifuroxazide (10 μM; Sigma-Aldrich) were applied 30 min before activation.

2.5 | Primary postnatal human microglia cultures

For the isolation of human microglia from surgical brain specimens (-Figure S3f), we essentially followed a previously published protocol (Rustenhoven et al., 2016). Briefly, blood vessels and meninges were removed from resected brain tissue using a dissection microscope (Zeiss Stemi DV4). Tissue was weighed, diced, and dissociated using the Neural Tissue Dissociation Kit (P) (#130–092-628, Miltenyi Biotec). Microglia were cultured as adherent cells in poly-L-lysin coated T75 tissue culture flasks in microglia culture medium containing DMEM/F12 (Gibco™, Thermo Fisher Scientific), 10% fetal calf serum (Biochrom, Merck) and 1X penicillin–streptomycin solution (Biochrom, Merck). After 1–2 weeks of culture in microglia culture medium at 37°C and 5% CO_2, cells were placed into multiwell plates for subsequent experiments (Figure S3g). To detach the cells, culture medium was removed and culture flasks were washed with phosphate buffered saline (PBS, without Mg++ and Ca++) followed by 5 min incubation with 3 ml Trypsin/EDTA solution (0.25%/0.02%; Biochrom, Merck) at 37 °C and 5% CO_2. To aid complete detachment, cells were gently scraped with a rubber cell scraper (Nunc, Thermo Fisher Scientific). After counting with a hemocytometer, cells were seeded in microglia culture medium at a density of 3.125×10^4 cells/cm². Further incubation overnight at 37°C and 5% CO_2 allowed attachment of cells and habituation to the new environment before the beginning of the activation experiments. The measurement times were chosen based on pilot tests studying a range of lithium concentrations (Figure S3a–c) and the time course of IDO1 protein expression after stimulation (Figure S3e). Purity of cultures was verified by immunostaining (Figure S2).

2.6 | Human induced pluripotent stem cells derived microglia

Differentiation of hiPSCs into hematopoietic progenitor cells (iHPCs) and subsequent differentiation of iHPCs into hiPSC-derived microglia was performed as described earlier (Abud et al., 2017). Briefly, hiPSCs were first differentiated into hematopoetic progenitor cells over a time period of 11 days using hematopoetic differentiation medium (HDM) containing IMDM (50%), F12 (50%), ITSG-X (2% v/v), Glutamax (1X), chemically-defined lipid concentrate (1X), non-essential amino acids (NEAA; 1X), Penicillin/Streptomycin (P/S; 1% V/V; all from Thermo Fisher Scientific), L-ascorbic acid 2-phosphate magnesium (64 μg/ml), monothioglycerol (400 μM), and PVA (10 μg/ml; all from Sigma). HDM was supplemented on day 0 with FGF2 (50 ng/ml; Peprotech), BMP4 (50 ng/ml; Miltenyi Biotec), Activin-A (12.5 ng/ml; Peprotech), RI (1 μm; Stem Cell Technology), and LiCl (2 mM; Sigma-Aldrich). Day 2 HDM was supplemented with FGF2 (50 ng/ml) and VEGF (50 ng/ml), days 4, 6, and 8 with FGF2 (50 ng/ml), VEGF (50 ng/ml), TPO (50 ng/ml), SCF (10 ng/ml), IL-6 (50 ng/ml), and IL-3 (10 ng/ml; all from Peprotech). Day 10 cells were harvested and FACsorted based on CD43 expression. CD43+ cells were transferred into microglia differentiation medium (MDM) containing phenol-free DMEM/F12 (1:1), ITS-G (2%v/v), B27 (2% v/v), N2 (0.5%, v/v; all from Thermo Fisher Scientific), monothioglycerol (200 μM), Glutamax (1X), NEAA (1X), and additional insulin (5 μg/ml; Sigma) for another 28 days. MDM contained the following supplements: Day 10–35: M-CSF (25 ng/ml), IL-34 (100 ng/ml), and TGFb-1 (50 ng/ml; all from Peprotech). Day 35–38: M-CSF (25 ng/ml), IL-34 (100 ng/ml), TGFb-1 (50 ng/ml), CD200 (100 ng/ml, Novoprotein), and CX3CL1 (100 ng/ml; Peprotech). After 38 days of differentiation, hiPSC derived microglia cells were harvested and seeded in 96 well plates (20,000 cells/well; Corning) containing MDM and M-CSF (25 ng/ml), IL-34 (100 ng/ml), TGFb-1 (50 ng/ml), CX3CL1 (100 ng/ml), and CD200 (100 ng/ml).

2.7 | Immunofluorescence and quantification

Cells were seeded onto poly-L-lysine precoated chamber slides (5000 cells/well; Sarstedt). Briefly, in preparation of staining, cells were washed three times with DPBS (1×) and then fixed with PFA (4% w/v) overnight at 4°C. Primary and secondary antibodies were diluted in TBS blocking buffer (96 ml 1×TBS, 1 ml 10% Triton X-100, 3 ml donkey serum). Primary antibodies were applied in the following concentrations: mouse anti-CD45 (EXBIO) 1:100, rabbit anti-IDO1 (Cell Signaling Technology) 1:100, rabbit anti-IBA1 (Wako Chemicals) 1:500, rabbit anti-PU.1 (Cell Signaling) 1:200, rabbit anti-TMEM119 (Biozol) 1:50, and rabbit anti-P2RY12 (Biozol) 1:50. Secondary antibodies coupled to different fluorochromes (Alexa488, Alexa647, Alexa488) were all from Invitrogen (Thermo Fisher Scientific). Secondary antibodies were used in a dilution of 1:400.

To measure mean fluorescence intensity of IDO1, Z-stack images were collected on an LSM 700 confocal microscope (Carl Zeiss). Consistent laser power and microscope settings were used across experiments. Zen® software (Carl Zeiss) was used for image analysis.

2.8 | Isolation of mRNA and quantitative polymerase chain reaction

RNA was isolated from cultured cells using the NucleoSpin® RNA XS kit (Macherey-Nagel). M-MLV reverse transcriptase and random hexamers

(both from Promega) were used for reverse transcription of RNA into cDNA. For polymerase chain reaction amplification, we used gene-specific primers and Light Cycler® 480 SYBR Green I Master (Roche Diagnostics). Polymerase chain reaction conditions were as follows: preincubation 95°C, 10 min, 95°C, 10 s, primer-specific annealing temperature, 10 s, 72°C, 15 s (45 cycles). Crossing points of amplified products were determined using the Second Derivative Maximum Method (Light Cycler Version LCS480 1.5.0.39, Roche). Quantification of messenger RNA expression was relative to receptor expression-enhancing protein 5 (*REEP5*; Eisenberg and Levanon (2013)). The specificity of polymerase chain reaction products was checked using melting curve analysis. PCR products were run on a 1.5% agarose gel to demonstrate the presence of a single amplicon of the correct size. Furthermore, negative controls (i.e., reaction mix lacking either template DNA or reverse transcriptase) yielded no bands on the gel.

2.9 | Western blot analysis

For protein extraction, cells were harvested in RIPA lysis buffer (150 mM NaCl, 5 mM EDTA, 1% NP-40, 1% sodium deoxycholate, 0.1% SDS, 25 mM Tris–HCl pH 7.6) containing phosphatase and protease inhibitors (PhosSTOP™, cOmplete™; both from Roche). Protein concentration was determined with the Pierce™ BCA Protein Assay Kit (Pierce™, Thermo Fisher Scientific). Equal amounts of protein were loaded on 10% SDS-polyacrylamide gels (Bio-Rad Laboratories) and blotted onto PVDF membranes (Immobilon, Millipore, Merck) for 150 min at 20 V. Blots were probed with primary and secondary antibodies and developed using near-infrared (NIR) fluorescence detection with Odyssey® CLx Imaging System (LI-COR). Equal loading of protein was confirmed by blotting against GAPDH or ACTB. Primary and secondary antibodies were applied in the following dilutions: IDO1 (1 mg/ml) 1:1000, GSK3β (Cell Signaling) 1:250, Phospho-GSK3β (Ser9; Cell Signaling) 1:250, STAT1 (Cell Signaling) 1:500, Phospho-STAT1 (Ser727; AAT Bioquest) 1:500, STAT3 (Cell Signaling) 1:500; Phospho-STAT3 (Tyr705; Cell Signaling) 1:500; GAPDH (Cell Signaling) 1:1000; ACTB (Abcam) 1:1000; IRDye® 800 (LI-COR) 1:10,000, and IRDye® 680 (LI-COR) 1:10,000.

2.10 | Intracellular immune cell signaling array

Cells were harvested in lysis buffer (Cell Signaling) and stored at −80°C until analysis. The PathScan® Immune antibody array kit (Cell Signaling) was used according to the manufacturer's instructions. Fluorescent images were acquired using the LI-COR® Biosciences Odyssey® imaging system. Fluorescence intensities for each spot were quantified using the LI-COR® Image Studio array analysis software and were depicted as in a heat map (LI-COR® Biosciences).

2.11 | Phagocytosis assay

To observe phagocytosis of bacterial particles, microglia cells cultured on PLL coated plasticware were incubated in live cell

imaging solution (Thermo Fisher Scientific) with pHrodo Red *Staphylococcus aureus* (Thermo Fisher Scientific) according to manufacturer's manual. After 2 h incubation at 37°C, Hoechst dye 33342 (2 μm; Abcam) was added for 10 min at 37°C, washed once with live cell imaging solution and imaged using an inverted fluorescence microscope (DMI 3000, Leica).

2.12 | MTT assay

Cell viability was assayed after 24 h incubation with LPS or IFN-γ as previously described (Uhlemann et al., 2016). The MTT labelling agent (Sigma-Aldrich) was added to the cells at a final concentration of 0.5 mg/ml. The converted dye was solubilized in 10% SDS in 0.01 M HCl and measured at 550 nm with a platereader (TriStar LB941, Berthold Technologies).

2.13 | Cytokine measurements

Cytokines in culture medium were measured using the Mesoscale MSD© Multi-Spot Assay System and the SECTOR Imager 6000 plate reader (both from Meso Scale Diagnostics) according to the manufacturer's instructions. All samples were run at least in duplicate.

2.14 | Chromatin immunoprecipitation

Chromatin for chromatin immunoprecipitation (ChIP) was prepared from immortalized human microglia using the Imprint® Chromatin Immunoprecipitation kit (Sigma-Aldrich) according to the manufacturer's instructions. Briefly, fragmented chromatin was immunoprecipitated with a ChIP-grade antibody against either STAT1 or STAT3 (both from BioLegend). Following reversal of cross-links and DNA precipitation, enriched DNA was analyzed by PCR amplification using a region-specific ChIP primer. QPCR data are presented as percent of input (%IP).

2.15 | Quantification of tryptophan and kynurenine concentrations

Cell culture medium (50 μl) was diluted three times with 0.3 M $HClO_4$ and centrifuged for 15 min at 13,000×g and 4 °C. Supernatant was transferred to a Spin-X® centrifuge tube filter (0.22 μm; Corning) and centrifuged at 5000×g for 5 min at 4°C. The flow-through was injected into the HPLC system. Kynurenine and tryptophan were analyzed by isocratic high-performance liquid chromatography (HPLC) using UltiMate 3000 pump and autosampler connected to a guard cell 5020 (+750 mV) and Coulochem III electrochemical detector with high sensitivity analytical cell 5011A (ECD1, +450 mV; ECD2, +700 mV; all from Thermo Fisher Scientific, Inc.). Both analytes were separated on a Hypersil™ BDS C18 column (150 mm, VDS-optilab)

using isocratic flow of the mobile phase MD-TM (Thermo Fisher Scientific) at a rate of 0.5 ml/min. Each run included standard curves of L-kynurenine and L-tryptophan (Sigma-Aldrich; diluted in 0.1 M HCl) with concentrations ranging from 10–500 ng/ml. For data acquisition and analysis, Chromeleon™ 7.2 Chromatography Data System (CDS) software was used (Thermo Fisher Scientific).

2.16 | Statistical analysis

Values are presented as mean ± SD. All statistical analyses were performed using GraphPad Prism 8 (GraphPad Software). Shapiro–Wilk test was used to confirm normal distribution of data. Unpaired t-test or two-way ANOVA were used to determine statistical significance.
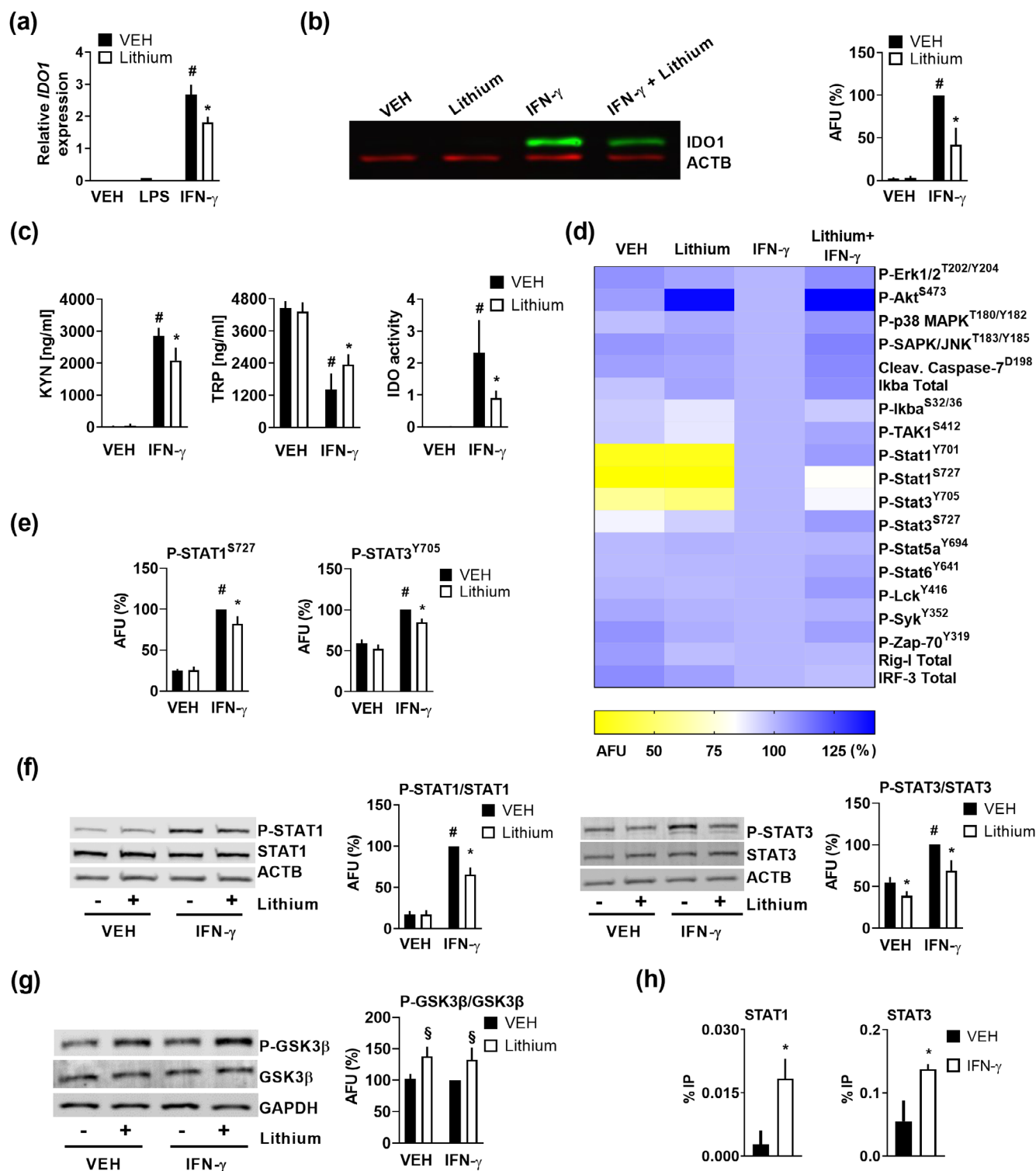

FIGURE 1 Legend on next page.

The results of relevant post hoc tests are given in the text. Percent effect was calculated relative to vehicle-treated controls (100%). $P < 0.05$ was considered statistically significant.

3 | RESULTS

3.1 | Lithium reduces microglial expression of IDO1 by inhibiting GSK3β, preventing STAT1/3 activation

To examine mRNA transcription of the first rate-limiting kynurenine pathway enzyme in response to TLR4 and type II interferon signaling, we treated a commercially available human microglia cell line with lipopolysaccharide (LPS) and IFN-γ for 12 h. We found that IFN-γ, but not LPS, was able to activate immortalized human microglia, inducing a robust *IDO1* mRNA increase which was significantly reduced when lithium was added to the cultures (Figure 1a; two-way ANOVA: lithium treatment, $F_{(1,18)} = 27.8$, $p < .0001$; LPS / IFN-γ activation, $F_{(2,18)} = 631.6$, $p < .0001$; interaction, $F_{(2,18)} = 22.1$, $p < .0001$; Tukey's post hoc test: [#] $p < .0001$ vehicle vs. IFN-γ, [*] $p < .0001$ IFN-γ vs. IFN-γ and lithium). Importantly, lithium (10 mM) did not exert toxic effects on microglia (Figure S1b). In contrast to *IDO1*, *IDO2* and *TDO* were not induced by IFN-γ treatment in immortalized human microglia (Figure S1e). To quantify intracellular protein levels, we performed a Western blot against IDO1 and β-actin (ACTB). IDO1 was only detectable after 12 h of IFN-γ, but not LPS treatment (Figure S1f), and the IDO1/ACTB ratio was significantly decreased (∼ 60%) in the presence of lithium (Figure 1b; two-way ANOVA: lithium treatment, $F_{(1,8)} = 24.46$, $p = .0011$; IFN-γ activation, $F_{(1,8)} = 141.1$, $p < .0001$; interaction, $F_{(1,8)} = 26.4$, $p = .0009$; Tukey's post hoc test: [#] $p < .0001$ vehicle vs. IFN-γ, [*] $p < .0005$ vehicle vs. IDO1 IFN-γ). Kynurenine (KYN) release into the cell culture medium was strongly increased by IFN-γ activation. Treatment with lithium significantly reduced this effect (Figure 1c; two-way ANOVA: lithium treatment, $F_{(1,12)} = 9.749$, $p = .0088$; IFN-γ activation, $F_{(1,12)} = 407.5$, $p < .0001$; interaction, $F_{(1,12)} = 10.71$, $p = .0067$; Tukey's post hoc test: [#] $p < .0001$ vehicle vs. IFN-γ, [*] $p < .0001$ IFN-γ vs. IFN-γ and lithium). Tryptophan (TRP) degradation increased massively after IFN-γ activation while co-treatment with lithium reduced tryptophan catabolism (Figure 1c;

two-way ANOVA: lithium treatment, $F_{(1,12)} = 3.817$, $p = .0744$; IFN-γ activation, $F_{(1,12)} = 146$, $p < .0001$; interaction, $F_{(1,12)} = 6.591$, $p = .0247$; Tukey's post hoc test: [#] $p < .0001$ vehicle vs. IFN-γ, [*] $p < 0.0452$ IFN-γ vs. IFN-γ and lithium). The ratio of KYN/TRP is an indirect measure of IDO activity. IDO activity was significantly reduced when IFN-γ stimulated immortalized human microglia were simultaneously incubated with lithium (Figure 1c; two-way ANOVA: lithium treatment, $F_{(1,12)} = 7.445$, $p = .0183$; IFN-γ activation, $F_{(1,12)} = 38.16$, $p < .0001$; interaction, $F_{(1,12)} = 7.541$, $p = .0177$; Tukey's post hoc test: [#] $p = .0002$ vehicle vs. IFN-γ, [*] $p = .0103$ IFN-γ vs. IFN-γ and lithium). Next, we aimed to investigate the pathway that might regulate IFN-γ induced *IDO1* transcription in human microglia cells. Overall, 19 signaling molecules involved in the regulation of immune and inflammatory responses were studied (Figure 1d). Three of the 19 signaling molecules studied showed strong induction in response to IFN-γ treatment for 1 h (P-STAT1[Y701], P-STAT1[S727], P-STAT3[Y705]), with lithium significantly reducing STAT1[S727] and STAT3[Y705] phosphorylation levels in IFN-γ treated cells (Figure 1e; two-way ANOVA for STAT1[S727]: lithium treatment, $F_{(1,16)} = 13.61$, $p = .002$; IFN-γ activation, $F_{(1,16)} = 766.1$, $p < .0001$; interaction, $F_{(1,16)} = 14.86$, $p = .0014$; two-way ANOVA for STAT3[Y705]: lithium treatment, $F_{(1,16)} = 34.13$, $p < .0001$; IFN-γ activation, $F_{(1,16)} = 397.1$, $p < .0001$; interaction, $F_{(1,16)} = 4.898$, $p = .0418$); Tukey's post hoc test: [#] $p < .0001$ vehicle vs. IFN-γ, [*] $p < .001$ IFN-γ vs. IFN-γ and lithium). Western blots against phosphorylated STAT1[S727] and STAT3[Y705] further corroborated this finding (Figure 1f; two-way ANOVA for STAT1[S727]: lithium treatment, $F_{(1,20)} = 58.69$, $p < .0001$; IFN-γ activation, $F_{(1,20)} = 842.3$, $p < 0.0001$; interaction, $F_{(1,20)} = 57.56$, $p < .0001$; two-way ANOVA for STAT3[Y705] lithium treatment, $F_{(1,20)} = 52.76$, $p < .0001$; IFN-γ activation, $F_{(1,20)} = 137.1$, $p < .0001$; interaction, $F_{(1,20)} = 5.779$, $p = .026$; Tukey's post hoc test: [#] $p < .0001$ vehicle vs. IFN-γ, [*] $p < .001$ IFN-γ vs. IFN-γ and lithium). Moreover, lithium increased GSK3β[S9] phosphorylation (Figure 1g, two-way ANOVA: lithium treatment, $F_{(1,20)} = 43.03$, $p < .0001$; IFN-γ activation, $F_{(1,20)} = .5572$, $p = .4641$; interaction, $F_{(1,20)} = .1112$, $p = .7422$; Tukey's post hoc test: [$] $p < .01$ vehicle vs. lithium for non- and IFN-γ- activated cells), resulting in inhibition of GSK3β activity (Jope & Johnson, 2004). Next, we performed chromatin immunoprecipitation to assess binding of STAT1 and STAT3 to the *IDO1* promoter. Primers spanning the STAT1, STAT3 binding site (−1086 bp relative to transcription start site according to Eukaryotic Promotor Database EPD, JASPAR CORE

FIGURE 1 Lithium suppresses IFN-γ induction of *IDO1* in immortalized human microglia by inhibiting STAT1 and STAT3 signaling. (a) *IDO1* mRNA expression was measured after LPS and IFN-γ activation. $N = 4$ independent experiments, [#] vehicle vs. IFN-γ, [*] IFN-γ vs. IFN-γ and lithium. (b) Representative Western blot analysis and relative fluorometric quantification after treatment with IFN-γ. AFU, arbitrary fluorescent units. Values are expressed as percentage of the IFN-γ-treatment condition (100%). $N = 3$ independent experiments, [#] vehicle vs. IFN-γ, [*] IFN-γ vs. IFN-γ and lithium. (c) The concentrations of kynurenine (KYN) and tryptophan (TRP) were measured after treatment with IFN-γ. The KYN/TRP ratio was used as a measure of IDO activity. $N = 4$ independent experiments, [#] vehicle vs. IFN-γ, [*] IFN-γ vs. IFN-γ and lithium. (d, e) After treatment with IFN-γ and/or lithium, an intracellular cell signaling antibody array (PathScan®) comprising a panel of 19 signaling molecules was performed. Lithium significantly reduced IFN-γ-induced phosphorylation of STAT1 at serine 727 as well as phosphorylation of STAT3 at tyrosine 705. $N = 5$ independent experiments, [#] vehicle vs. IFN-γ, [*] IFN-γ vs. IFN-γ and lithium. (f) Western blots confirming the results of the PathScan® analysis. $N = 6$ independent experiments, [#] IFN-γ vs. vehicle, [*] IFN-γ vs. IFN-γ and lithium. (g) Lithium increases phosphorylation of GSK3β. $N = 6$ independent experiments, § $p < .01$ IFN-γ vs. IFN-γ and lithium as well as vehicle vs. vehicle and lithium. (h) Real-time PCR analysis of *IDO1* promoter fragments recovered in chromatin immunoprecipitation (ChIP) experiments with antibodies against STAT1 and STAT3. Chromatin was prepared after treatment with IFN-γ. Quantitative PCR data are presented as percent of input (%IP). $N = 3$, [*] $p < .05$
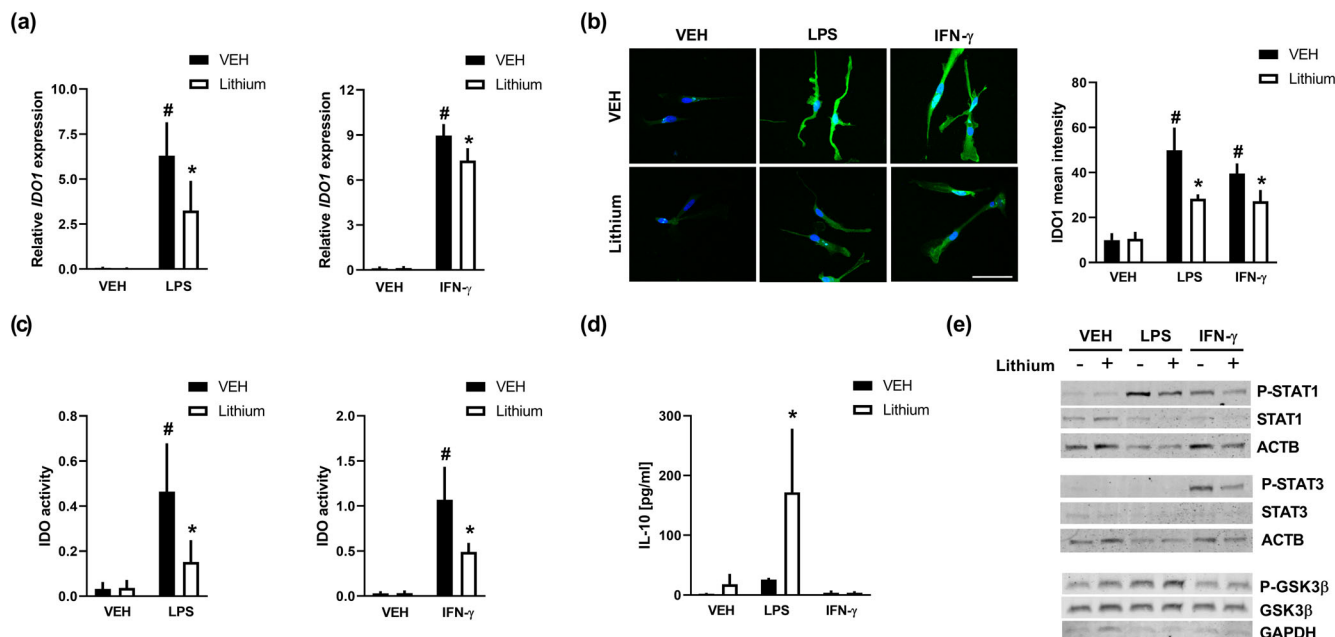
FIGURE 2 Lithium reduces kynurenine pathway activity in activated primary human microglia. (a) *IDO1* mRNA expression was measured after stimulation with LPS or IFN-γ. $N = 4$ independent experiments (i.e., primary cells from four different surgical specimens), [#] vehicle vs. stimulation condition, [*] stimulation condition vs. stimulation condition with lithium. (b) Representative immunofluorescent images demonstrating that IDO1 protein expression (green) is increased after treatment with either LPS (upper middle image) or IFN-γ (upper right image). The bottom images show that lithium reduced this increase in IDO1 in activated microglia. Blue, Hoechst nuclear counterstain. Green fluorescence intensity (i.e., IDO1 expression) was quantified using Zen® software. Microglia from a single surgical specimen were used. Five images containing between 2 and 11 microglia cells each were analyzed per condition. Mean fluorescence intensity was calculated for each image ($n = 5$), [#] vehicle versus stimulation condition, [*] stimulation condition versus stimulation condition with lithium. (c) IDO1 activity was quantified as KYN/TRP ratio. $N = 5$ independent experiments (i.e., primary cells from five different surgical specimens), [#] vehicle vs. stimulation condition, [*] effect of lithium in stimulated microglia. Two-way ANOVA followed by Tukey's post hoc test. (d) IL-10 protein concentration was measured in cell culture supernatant. $N = 4$ independent experiments (i.e., primary cells from four different surgical specimens), [*] LPS vs. LPS and lithium. (e) Representative Western blots confirming the results obtained in immortalized human microglia. Note that, unlike immortalized human microglia, primary human microglia can be activated by both LPS and IFN-γ

vertebrates) were used. Enriched binding of both STAT1 and STAT3 to the *IDO1* promoter was observed after 3 h IFN-γ activation of immortalized human microglia cells (Figure 1h; unpaired *t* test: [*] $p < .05$).

3.2 | Lithium reduces kynurenine pathway activity in activated primary human microglia

Since immortalized human microglia proved insensitive to LPS, *IDO1* transcription was further investigated in primary human microglia. These primary cells were cultured from cortical brain biopsies of patients suffering from temporal lobe epilepsy. Cultures expressed typical microglia markers such as IBA1, PU.1, TMEM119, CD45, and P2YR12 (Figure S2a). Moreover, these cells phagocytosed bacterial particles and retained a rod-shaped morphology even after activation with IFN-γ or LPS (Figure S2b, c), which is in contrast to the amoeboid shape observed after LPS treatment in postnatal primary mouse microglia (Bronstein et al., 2013; Tam & Ma, 2014). LPS and IFN-γ (Figure 2a, 24 h) were both found to be strong inducers of *IDO1* mRNA transcription in primary human microglia. Lithium co-treatment significantly reduced this effect (Figure 2a; two-way ANOVA for LPS: lithium treatment, $F_{(1,12)} = 6.089$, $p = .0296$; LPS

activation, $F_{(1,12)} = 57.94$, $p < .0001$; interaction, $F_{(1,12)} = 5.99$, $p = .0331$; two-way ANOVA for IFN-γ: lithium treatment, $F_{(1,12)} = 8.416$, $p = .0133$; IFN-γ activation, $F_{(1,12)} = 256.5$, $p < .0001$; interaction, $F_{(1,12)} = 8.554$, $p = .0127$; Tukey's post hoc test: [#] $p < .0001$ vehicle vs. LPS or IFN-γ, [*] $p < .05$ LPS or IFN-γ vs. LPS or IFN-γ and lithium). MTT assay confirmed that lithium was non-toxic to primary human microglia at the concentration of 10 mM (Figure S3b). There was no apparent regulation of either *IDO2* or *TDO* in primary human microglia in response to stimulation with LPS or IFN-γ, the levels of both transcripts being just above the detection limit (Figure S3d). To evaluate IDO1 protein expression in primary human microglia, we performed immunocytochemistry and measured fluorescence intensities. IDO1 became detectable after 12 h stimulation of primary human microglia with either LPS or IFN-γ (Figure S3e) and was further analyzed at 24 h (Figure 2b). Again, co-treatment with lithium reduced IDO1 expression (Figure 2b; two-way ANOVA: activation with LPS or IFN-γ, $F_{(2,24)} = 82.88$, $p < .0001$; lithium treatment, $F_{(1,24)} = 32.91$, $p < .0001$; interaction, $F_{(2,24)} = 10.91$, $p = .0004$; Tukey's post hoc test: [#] $p < .0001$ vehicle vs. LPS or IFN-γ, [*] $p < .05$ LPS or IFN-γ vs. LPS or IFN-γ and lithium). Furthermore, IDO activity in primary human microglia was investigated following 24 h treatment with LPS or IFN-γ (Figure 2c). The kynurenine/
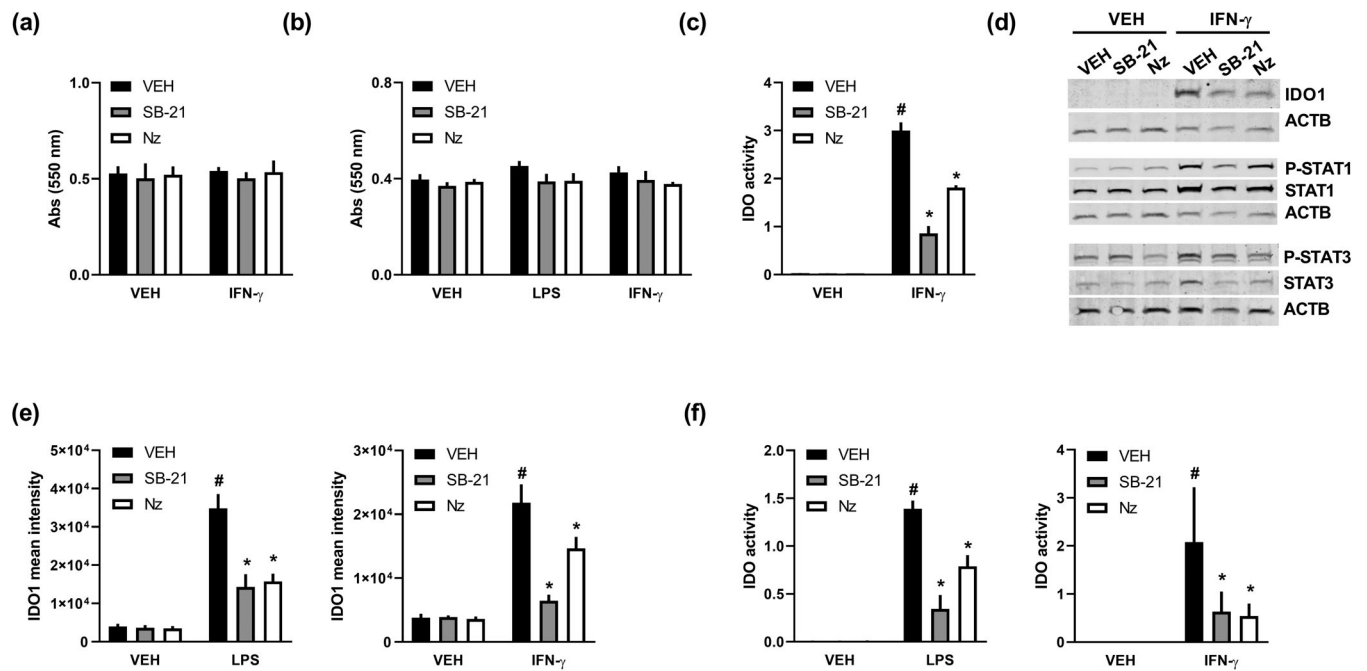
FIGURE 3 Inhibitors of GSK3β and STAT are able to modulate IDO activity in immortalized and primary human microglia. (a, b) Cell viability following treatment with GSK3 inhibitor SB-216763 (SB-21), STAT inhibitor nifuroxazide (Nz), or vehicle was studied using MTT assay. (a) Immortalized human microglia and (b) primary human microglia. $N = 3$ independent experiments. (c) HPLC analysis of cell culture supernatant to assess IDO activity in immortalized human microglia. Analyses were performed after stimulation with IFN-γ and co-treatment with either SB-21, Nz, or vehicle. $N = 3$ independent experiments, [#] vehicle vs. IFN-γ, [*] IFN-γ vs. IFN-γ and co-treatment with either inhibitor. (d) Western blot of cell extracts of immortalized human microglia. IDO1 expression was studied after IFN-γ treatment. STAT1, STAT3 as well as phosphorylation of STAT1 at serine 727 and phosphorylation of STAT3 at tyrosine 705 were assessed following IFN-γ stimulation. β-Actin (ACTB) was used as a loading control. (e) IDO1 expression in primary human microglia was quantified based on fluorescence intensity. Microglia from a single surgical specimen were used. $N = 5$, [#] vehicle vs. LPS or IFN-γ, [*] LPS or IFN-γ vs. LPS or IFN-γ and co-treatment with an inhibitor. (f) HPLC analysis of cell culture supernatant to assess IDO activity in primary human microglia. $N = 3$ independent experiments (i.e., primary cells from three different surgical specimens), [#] vehicle vs. LPS or IFN-γ, [*] LPS or IFN-γ vs. LPS or IFN-γ and co-treatment with either inhibitor

tryptophan ratio was studied in primary cells derived from 4 different individuals. While LPS and IFN-γ increased IDO activity, the addition of lithium to the cultures significantly reduced this effect (Figure 2c; two-way ANOVA for LPS: lithium treatment, $F_{(1,16)} = 8.228$, $p = .0111$; LPS activation, $F_{(1,16)} = 26.05$, $p = .0001$; interaction, $F_{(1,16)} = 8.661$, $p = .0096$; two-way ANOVA for IFN-γ: lithium treatment, $F_{(1,16)} = 11.35$, $p = .0039$; IFN-γ activation, $F_{(1,16)} = 76.57$, $p < .0001$; interaction, $F_{(1,16)} = 11.51$, $p = .0037$; Tukey's post hoc test: [#] $p < .001$ vehicle vs. LPS or IFN-γ, [*] $p < .01$ LPS or IFN-γ vs. LPS or IFN-γ and lithium). Since lithium has well-known anti-inflammatory properties (Huang et al., 2009; Nahman et al., 2012; Yuskaitis & Jope, 2009), we also measured the expression of anti-inflammatory cytokine IL-10. We found IL-10 to be specifically induced in microglia after 24 h LPS and lithium treatment. Co-treatment with lithium caused a massive increase in IL-10 levels of more than four times the levels observed in LPS-stimulated cells (Figure 2d; two-way ANOVA: activation with LPS or IFN-γ, $F_{(2,18)} = 11.60$, $p = .006$; lithium treatment, $F_{(1,18)} = 9.032$, $p = .0076$; interaction, $F_{(2,18)} = 6.612$, $p = .007$; Tukey's post hoc test: [*] $p < .01$ LPS vs. LPS and lithium). In a next step, we investigated the phosphorylation status of transcriptional regulators STAT1 und STAT3 (Figure 2e). Given the limited availability of primary cells, the expression of STAT1 and STAT3 was close to the Western blot detection limit in our experiments.

However, primary human microglia showed a clear increase in phosphorylation of STAT1^S727 after 1 h activation with LPS (Figure 2e, top). IFN-γ activation (1 h) increased phosphorylation of both STAT1^S727 and STAT3^Y705 (Figure 2e, top and center). Furthermore, dephosphorylation of STAT1^S727 and STAT3^Y705 was clearly apparent after lithium treatment of IFN-γ activated primary human microglia (Figure 2e). Finally, GSK3β is constitutively expressed at a high level in primary human microglia. Again, lithium increased inhibitory phosphorylation at serine 9 (Figure 2e, bottom).

3.3 | Inhibitors of GSK3β and STAT are able to modulate IDO activity in immortalized and primary human microglia

Next, we investigated whether modulation of GSK3β and STAT activity alters microglia function and IDO activity. SB-216763 (SB-21) was used to inhibit GSK3β activity (Coghlan et al., 2000). Nifuroxazide (Nz) was used to inhibit STAT signaling (Nelson et al., 2008). MTT assays, performed after 24 h, confirmed that, at the concentrations used in subsequent experiments, inhibitors did not affect cell viability of immortalized (Figure 3a; two-way ANOVA: inhibitor treatment,
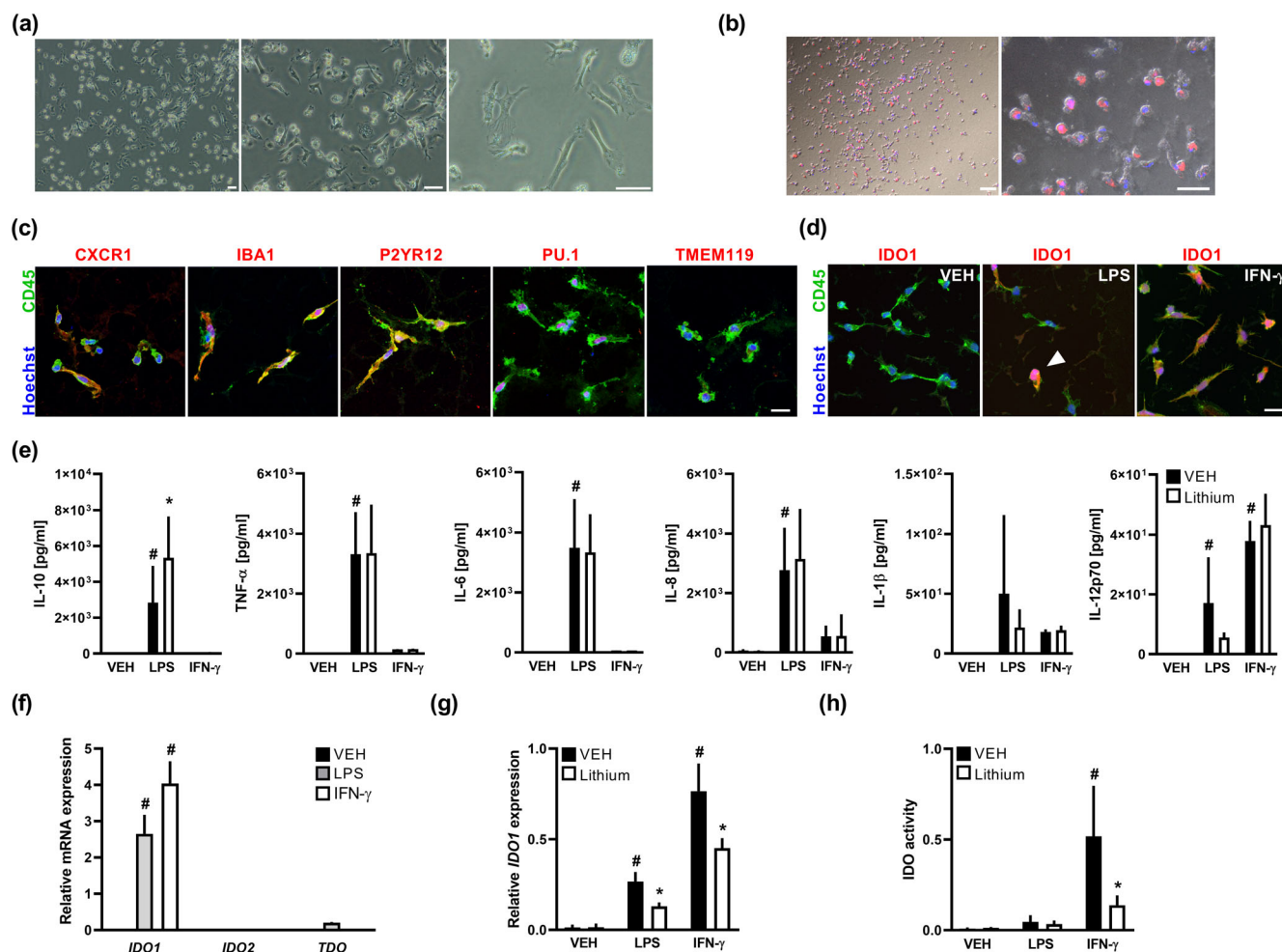
FIGURE 4 Tryptophan catabolism in hiPSC-derived microglia. (a) Representative brightfield images of hiPSC-derived microglia. Scale bar: 50 μm. (b) Live cell images of hiPSC-derived microglia phagocytosing bacterial particles (red), blue: nuclear stain Hoechst 33342. Brightfield and fluorescence images were merged into a composite image. Scale bar left: 100 μm, right: 50 μm. (c) Representative confocal images of differentiated hiPSC-derived microglia-like cells demonstrate expression of typical microglia markers such as CD45, CXCR1, P2YR12, IBA1, and PU.1, but not TMEM119. Hoechst 33342 was used as nuclear counterstain. Scale bar: 20 μm. (d) IDO1 protein expression is strongly induced in IFN-γ stimulated cells. Scale bar: 20 μm. (e) Microglia-like cells derived from hiPSCs show typical release of pro-inflammatory cytokines after LPS treatment. HiPSC-derived microglia cells from three different donor cell lines (BIHi005-A, BIHi004-A, and BIHi001-A) were used ($n = 3$ experiments), # $p < 0.05$ vehicle vs. LPS or IFN-γ, * LPS vehicle vs. LPS and co-treatment with lithium. (f) *IDO1*, *IDO2*, and *TDO* mRNA expression in differentiated hiPSC-derived microglia-like cells after LPS or IFN-γ treatment. Significant regulation was only observed for *IDO1*. $N = 3$ experiments from hiPSC cell line BIH-004; # vehicle vs. LPS or IFN-γ. (g) *IDO1* mRNA following stimulation with LPS or IFN-γ and co-treatment with lithium. $N = 3$ experiments from three different donor cell lines (BIHi005-A, BIHi004-A, and BIHi001-A), # vehicle vs. LPS or IFN-γ, * LPS or IFN-γ vs. LPS or IFN-γ and co-treatment with lithium. (h) IDO activity following LPS or IFN-γ treatment, $n = 3$ experiments from three different donor cell lines (BIHi005-A, BIHi004-A, and BIHi001-A), # vehicle vs. IFN-γ, * IFN-γ vs. IFN-γ and co-treatment with lithium

$F_{(2,12)} = .7254$, $p = .5042$; IFN-γ activation, $F_{(1,12)} = .1453$, $p = .7097$; interaction, $F_{(2,12)} = .0421$, $p = .959$) or primary human microglia (Figure 3b; two-way ANOVA: inhibitor treatment, $F_{(2,18)} = 7.993$, $p = .0033$; LPS/IFN-γ activation, $F_{(2,18)} = 2.526$, $p = .1097$; interaction, $F_{(4,18)} = 1.15$, $p = .365$; Tukey's post hoc test: no significant interaction between vehicle vs. inhibitor treatment within VEH, LPS or IFN-γ activated cells). Activity measurements revealed that both SB-216763 and nifuroxazide significantly reduced IDO activity in immortalized human microglia stimulated with IFN-γ for 24 h (Figure 3c; two-way ANOVA: inhibitor treatment, $F_{(2,12)} = 189.6$, $p < .0001$; IFN-γ activation, $F_{(1,12)} = 1716$, $p < .0001$; interaction,

$F_{(2,12)} = 188.5$, $p < .0001$; Tukey's post hoc test: # $p < .0001$ vehicle vs. IFN-γ, * $p < .0001$ IFN-γ vs. IFN-γ and inhibitor). IDO1 protein expression in IFN-γ activated immortalized cells was significantly reduced by 12 h inhibitor treatment (Figure 3d). To further elucidate the effects of SB-216763 and nifuroxazide on the regulation of IDO1, we investigated whether phosphorylation of STAT1[S727] and STAT3[Y705] would be modulated by either compound following 1 h stimulation with LPS or IFN-γ. The results of Western blots indicated that treatment with SB-216763 reduced P-STAT1[S727] and P-STAT3[Y705]. Treatment with nifuroxazide inhibited P-STAT3[Y705] (Figure 3d). Finally, in primary human microglia, 24 h inhibitor

treatment of LPS or IFN-γ activated cells resulted in significantly reduced IDO1 protein expression (Figure 3e; two-way ANOVA for LPS: inhibitor treatment, $F_{(2,24)} = 66.82$, $p < .0001$; LPS activation, $F_{(1,24)} = 472.3$, $p < .0001$; interaction, $F_{(2,24)} = 61.6$, $p < .0001$; two-way ANOVA for IFN-γ: inhibitor treatment, $F_{(2,24)} = 67.31$, $p < .0001$; IFN-γ activation, $F_{(1,24)} = 384.2$, $p < .0001$; interaction, $F_{(2,24)} = 68.98$, $p < .0001$; Tukey's post hoc test: $^{\#}$ $p < .0001$ vehicle vs. LPS or IFN-γ, * $p < .0001$ LPS or IFN-γ vs. LPS or IFN-γ and lithium) and reduced IDO activity (Figure 3f; two-way ANOVA for LPS: inhibitor treatment, $F_{(2,12)} = 59.35$, $p < .0001$; LPS activation, $F_{(1,12)} = 449.8$, $p < .0001$; interaction, $F_{(2,12)} = 59.79$, $p < .0001$; two-way ANOVA for IFN-γ: inhibitor treatment, $F_{(2,12)} = 4.352$, $p = .0379$; IFN-γ activation, $F_{(1,12)} = 20.34$, $p = .0007$; interaction, $F_{(2,12)} = 4.366$, $p = .0376$; Tukey's post hoc test: $^{\#}$ $p < .01$ vehicle vs. LPS or IFN-γ, * $p < .05$ LPS or IFN-γ vs. LPS or IFN-γ and lithium).

3.4 | Tryptophan metabolism in human induced pluripotent stem cell-derived microglia

Considering the limited availability of human primary cells, we also studied tryptophan metabolism in hiPSC-derived microglia using three different human iPSC lines. Human iPSC-derived microglia were differentiated according to an existing protocol (Abud et al., 2017). This method produces pure cultures with characteristic rod-shaped cells (Figure 4a). These cells phagocytose bacterial particles (Figure 4b) and express typical microglia markers such as CXCR1, IBA1, P2YR12, PU.1, and CD45, but not TMEM119 (Figure 4c). IDO1 immuno-staining showed that all cells expressing CD45 after IFN-γ stimulation also expressed the IDO1 protein. By contrast, IDO1 immunoreactivity was not found in all cells after LPS activation (Figure 4d). However, 24 h LPS treatment of hiPSC-derived microglia resulted in activation of cytokines IL-10, TNF-α, IL-6, IL-8, and IL-12p70 (Figure 4e; two-way ANOVA for IL-10: lithium treatment, $F_{(1,12)} = 1.973$, $p = .1816$; LPS/IFN-γ activation, $F_{(2,12)} = 20.85$, $p = .0001$; interaction, $F_{(2,12)} = 1.973$, $p = .1816$; two-way ANOVA for TNF-α: lithium treatment, $F_{(1,12)} = 0.0014$, $p = .9705$; LPS/IFN-γ activation, $F_{(2,12)} = 27.84$, $p < .0001$; interaction, $F_{(2,12)} = 0.0008$, $p = .9992$; two-way ANOVA for IL-6: lithium treatment, $F_{(1,12)} = 0.0161$, $p = .9014$; LPS/IFN-γ activation, $F_{(2,12)} = 32.06$, $p < .0001$; interaction, $F_{(2,12)} = 0.0149$, $p = .9853$; two-way ANOVA for IL-8: lithium treatment, $F_{(1,12)} = 0.0784$, $p = .7842$; LPS/IFN-γ activation, $F_{(2,12)} = 15.76$, $p = .0004$; interaction, $F_{(2,12)} = 0.0755$, $p = .9277$; two-way ANOVA for IL-1β: lithium treatment, $F_{(1,12)} = 0.4714$, $p = .5054$; LPS/IFN-γ activation, $F_{(2,12)} = 2.458$, $p = .1274$; interaction, $F_{(2,12)} = 0.551$, $p = .5903$; two-way ANOVA for IL-12p70: lithium treatment, $F_{(1,12)} = 0.3074$, $p = .5895$; LPS / IFN-γ activation, $F_{(2,12)} = 40.17$, $p < .0001$; interaction, $F_{(2,12)} = 1.712$, $p = .2218$; uncorrected Fisher's LSD post hoc test: $^{\#}$ $p < .05$ vehicle vs. LPS or IFN-γ, * $p < .05$ LPS or IFN-γ vs. LPS or IFN-γ and lithium). The significant upregulation of IL-10 in LPS activated primary cells in the presence of lithium was recapitulated in hiPSC-derived microglia (Figure 2d and Figure 4e). Gene expression analyses of tryptophan degrading enzymes IDO1, IDO2, and TDO were performed. Stimulation with LPS or IFN-γ for

24 h resulted in strong upregulation of IDO1 mRNA transcription with no significant effects on IDO2 or TDO (Figure 4f; two-way ANOVA: mRNA expression, $F_{(2,18)} = 200.1$, $p < .0001$; LPS / IFN-γ activation, $F_{(2,18)} = 59.85$, $p < .0001$; interaction, $F_{(4,18)} = 57.77$, $p < .1816$; uncorrected Fisher's LSD post hoc test: $^{\#}$ $p < .0001$ vehicle vs. LPS or IFN-γ). Finally, lithium treatment decreased IDO1 mRNA transcription after 6 h LPS or IFN-γ activation (Figure 4g; two-way ANOVA: lithium treatment, $F_{(1,12)} = 20.10$, $p = .0007$; LPS/IFN-γ activation, $F_{(2,12)} = 110.1$, $p < .0001$; interaction, $F_{(2,12)} = 7.435$, $p < .0079$; uncorrected Fisher's LSD post hoc test: $^{\#}$ $p < .001$ vehicle vs. LPS or IFN-γ, * $p < .05$ LPS or IFN-γ vs. LPS or IFN-γ and lithium). Increased IDO activity was found after IFN-γ activation, an effect which was again attenuated by lithium (Figure 4h; two-way ANOVA: lithium treatment, $F_{(1,12)} = 5.472$, $p = .0374$; LPS/IFN-γ activation, $F_{(2,12)} = 13.39$, $p < .0009$; interaction, $F_{(2,12)} = 5.149$, $p < .0243$; uncorrected Fisher's LSD post hoc test: $^{\#}$ $p < .001$ vehicle vs. IFN-γ, * $p < .05$ IFN-γ vs. IFN-γ and lithium).

4 | DISCUSSION

The biological mechanisms underpinning lithium therapy are not clearly understood. One of the most robust and consistent findings reported in the literature and replicated here is that lithium inhibits glycogen synthase kinase (GSK)3β (Chalecka-Franaszek & Chuang, 1999; Klein & Melton, 1996; Stambolic et al., 1996), a ubiquitous serine/threonine kinase with particularly high expression in brain (Woodgett, 1990). A number of clinical studies have demonstrated an increase in 5-hydroxyindoleacetic acid (5-HIAA), the main serotonin metabolite, in cerebrospinal fluid (CSF) of patients receiving lithium (Berrettini et al., 1985; Bowers & Heninger, Bowers Jr. & Heninger, 1977; Fyro et al., 1975). Co-prescription of lithium and serotonergic antidepressants heightens the risk of serotonin toxicity (Adan-Manes et al., 2006; Prakash et al., 2017; Sobanski et al., 1997). Furthermore, accumulating evidence has linked higher-lethality suicide attempts to central serotonin system hypofunction (e.g., Asberg et al. (1976); Mann et al. (1989); Roy et al. (1989); Sullivan et al. (2015)), whereas lithium has proven anti-suicidal properties (Cipriani et al., 2013). Based on these findings, it has long been suspected that part of lithium's benefit might be mediated directly via serotonin (Muller-Oerlinghausen, 1985). Against this background, our study was designed to investigate in microglia, the brain's resident immune cells, the effect of lithium on the inflammation-induced kynurenine pathway, which siphons tryptophan away from serotonin biosynthesis.

Microglia are the main effector cell driving the brain's innate immune response. As such, microglia are an important first line of defense and lend themselves well as a cellular target for strategies aimed at modulating neuroinflammation (Colonna & Butovsky, 2017). To our knowledge, this is the first report documenting the effect of lithium on kynurenine-pathway activity in microglia.

Considerable doubt has been raised as to whether mice are suitable to model inflammation observed in human patients (Seok et al., 2013).

Notwithstanding the extra labor involved, the experiments reported herein were therefore conducted in human-derived cells. Cell culture models are inherently reductionist, being composed of only one cell type investigated ex vivo under non-physiological conditions for a necessarily relatively short period. The attendant difficulties and limitations should be clearly acknowledged. Not infrequently, the pace of such experiments in the dish exceeds by far the speed with which the corresponding effects become observable in vivo. As concerns microglia cultures in particular, in the interest of reasonably quick and reproducible experiments, biomolecules and pharmacological agents are typically applied to cells at rather high concentrations, the equivalents of which would not usually be used in experimental animals or expected to be seen in the human brain unless in most severe disease. This is certainly true for the concentrations of LPS and IFN-γ used herein for a short span of just 24 h in line with numerous prior studies (Carrillo-Jimenez et al., 2019; Frugier et al., 2010; Huang et al., 2009; Nguyen et al., 2017). It should also be noted that the effects of lithium investigated in our experiments all relate to intracellular signaling and that IDO1, one of whose main evolutionary roles seems to have been to starve intracellular pathogens of tryptophan, is a cytosolic protein lacking a known secreted isoform (Schmidt & Schultze, 2014; van Baren & an den Eynde, 2015). The intracellular concentration of lithium in microglia of experimental animals or human patients receiving therapeutic lithium salts remains to be established. Moreover, it should not go unmentioned that a recent study using [7]Li MR imaging found significant heterogeneity in lithium distribution within the brain of subjects with bipolar disorder with particularly high signal intensity found, most remarkably, in the brain stem (Smith et al., 2018). Further, [7]Li MR spectroscopy suggests that an extensive fraction of lithium resides in the intracellular compartment in the human brain in vivo, albeit with estimates falling within a broad range (Komoroski et al., 1997). Finally, a steady-state concentration of lithium (i.e., an intracellular concentration producing stable therapeutic effects) is only achieved in vivo after four to 5 days (Ward et al., 1994). Against this complex backdrop, we were guided in our choice of lithium concentration primarily by the previous literature on lithium effects in microglia and glial cells in culture and proceeded after having confirmed good tolerability using the MTT assay (e.g., Cao et al., 2017; Davenport et al., 2010; Feinstein, 1998; Yuskaitis & Jope, 2009; Zheng et al., 2017).

Our study establishes a signaling pathway by which lithium inhibits inflammatory activation of the kynurenine pathway in human microglia (Figure 5). The effects of lithium were corroborated using multiple readouts including mRNA and protein expression as well as the KYN/TRP ratio.

Glycogen synthase kinase 3β (GSK3β) plays a central role in regulating the cellular immune response. In line with the existing literature, we confirmed inhibitory phosphorylation of GSK3β at serine 9 in human microglia treated with lithium (Stambolic et al., 1996; Sutherland et al., 1993). In mice, GSK3β activation after stimulation with IFN-γ has been shown to lead to downstream phosphorylation of STAT1 at serine 727 (Tsai et al., 2009) and STAT3 at tyrosine 705 (Beurel & Jope, 2008). Using an antibody array to interrogate our samples, we confirmed this inflammatory signaling cascade in human cells. Importantly, enriched binding of both STAT1 and STAT3 to the IDO1 promoter was observed after IFN-γ activation of immortalized human microglia cells. Further, we identified dephosphorylation of
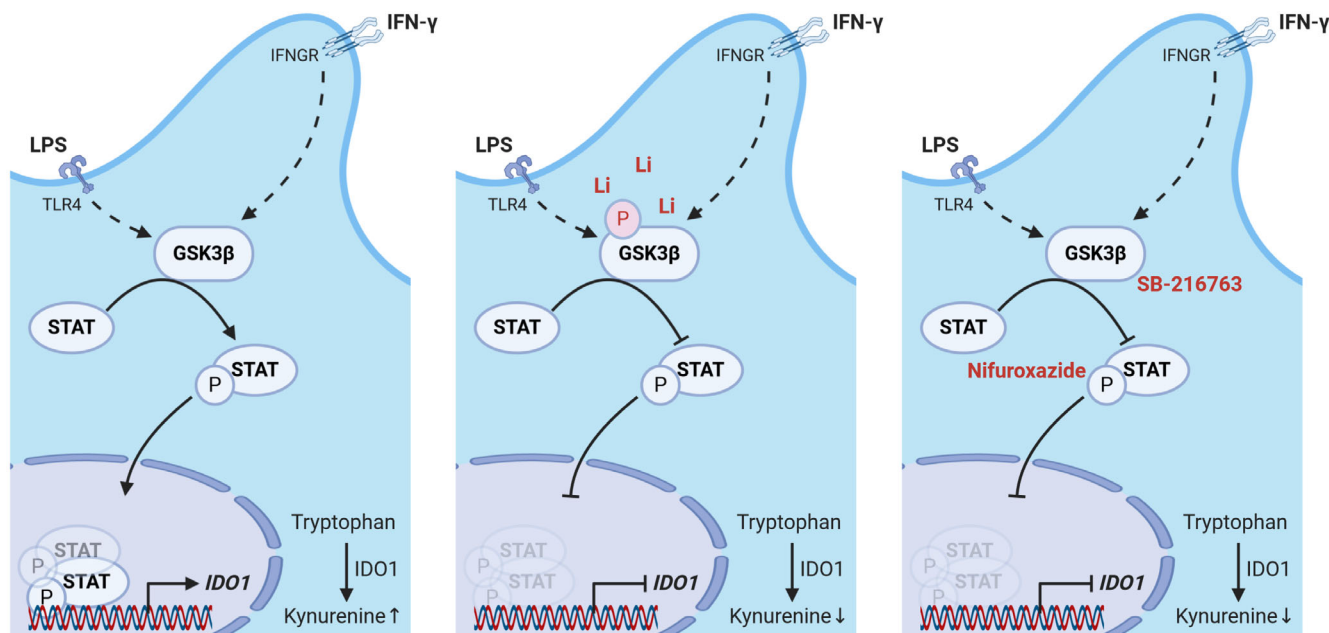

FIGURE 5 Lithium inhibits tryptophan catabolism along the kynurenine pathway in activated human microglia. When microglia become activated in response to stimulation of toll-like receptor 4 (TLR4) or the IFN-γ receptor (IFNGR), GSK3β phosphorylates STAT1 at serine 727 and STAT3 at tyrosine 705, allowing dimerization, nuclear translocation, and inflammation-induced IDO1 mRNA transcription. Lithium phosphorylates GSK3β at serine 9, thereby blocking the crucial role of GSK3β in microglia activation. GSK3β inhibitor SB-216763 and STAT inhibitor nifuroxazide recapitulate the effects of lithium on IDO1 mRNA transcription. Created with BioRender.com

STAT1 at serine 727 and STAT3 at tyrosine 705 as the principal signaling route of lithium, blocking nuclear translocation and DNA binding of these transcription factors in response to inflammatory activation (Darnell et al., 1994). Crucially, we were able to show that pharmacological inhibition of GSK3 and STAT recapitulates lithium's inhibitory effect on the kynurenine pathway.

Taken together, immortalized human microglia, primary human microglia harvested from surgical specimens, and microglia-like cells differentiated from human iPSCs lend themselves well to modeling key features of neuroinflammation. The main difference between the three cell types relates to stimulation with LPS, which produced marked induction of IDO1 in primary microglia, showed some upregulation in hiPSC-derived cells, but yielded virtually no response in the immortalized human microglia cell line investigated. *IDO1* mRNA and protein expression as well as IDO activity were robustly induced after stimulation with IFN-γ.

In sum, lithium counteracts tryptophan catabolism along the kynurenine pathway in stimulated human-derived microglia by increasing inhibitory GSK3β^{S9} phosphorylation and reducing, in turn, STAT1^{S727} and STAT3^{Y705} phosphorylation levels. Although lithium is a highly pleiotropic agent that interacts with multiple intracellular signaling pathways, we speculate that inhibition of inflammation-induced tryptophan breakdown explains critical aspects of lithium's clinical and pharmacological properties.

AUTHOR CONTRIBUTION

G.K., R.G., and K.G. conceived this study. R.G. performed the experiments. R.G., G.K. and K.G. analyzed the data. P.F., U.C.S. and L.K. collected human brain tissue. G.K., K.G. and R.G. wrote the manuscript with input from all authors. All authors discussed the results and commented on the final manuscript.

CONFLICT OF INTEREST

The authors declare no conflict of interest.

DATA AVAILABILITY STATEMENT

The data used to support these findings are available from the corresponding author upon reasonable request.

ORCID

Ria Göttert https://orcid.org/0000-0003-4756-7381

REFERENCES

Abud, E. M., Ramirez, R. N., Martinez, E. S., Healy, L. M., Nguyen, C. H. H., Newman, S. A., Yeromin, A. V., Scarfone, V. M., Marsh, S. E., Fimbres, C., Caraway, C. A., Fote, G. M., Madany, A. M., Agrawal, A., Kayed, R., Gylys, K. H., Cahalan, M. D., Cummings, B. J., Antel, J. P., ... Blurton-Jones, M. (2017). iPSC-derived human microglia-like cells to study neurological diseases. *Neuron*, *94*(2), 278–293 e279. https://doi.org/10.1016/j.neuron.2017.03.042

Adan-Manes, J., Novalbos, J., Lopez-Rodriguez, R., Ayuso-Mateos, J. L., & Abad-Santos, F. (2006). Lithium and venlafaxine interaction: A case of serotonin syndrome. *Journal of Clinical Pharmacy and Therapeutics*, *31*(4), 397–400. https://doi.org/10.1111/j.1365-2710.2006.00745.x

Ajmone-Cat, M. A., D'Urso, M. C., di Blasio, G., Brignone, M. S., De Simone, R., & Minghetti, L. (2016). Glycogen synthase kinase 3 is part of the molecular machinery regulating the adaptive response to LPS stimulation in microglial cells. *Brain, Behavior, and Immunity*, *55*, 225–235. https://doi.org/10.1016/j.bbi.2015.11.012

Asberg, M., Traskman, L., & Thoren, P. (1976). 5-HIAA in the cerebrospinal fluid. A biochemical suicide predictor? *Archives of General Psychiatry*, *33*(10), 1193–1197. https://doi.org/10.1001/archpsyc.1976.01770100055005

Bauer, M., Adli, M., Bschor, T., Pilhatsch, M., Pfennig, A., Sasse, J., ... Lewitzka, U. (2010). Lithium's emerging role in the treatment of refractory major depressive episodes: Augmentation of antidepressants. *Neuropsychobiology*, *62*(1), 36–42. https://doi.org/10.1159/000314308

Berrettini, W. H., Nurnberger, J. I., Jr., Scheinin, M., Seppala, T., Linnoila, M., Narrow, W., Simmons-Alling, S., & Gershon, E. S. (1985). Cerebrospinal fluid and plasma monoamines and their metabolites in euthymic bipolar patients. *Biological Psychiatry*, *20*(3), 257–269. https://doi.org/10.1016/0006-3223(85)90055-1

Beurel, E., & Jope, R. S. (2008). Differential regulation of STAT family members by glycogen synthase kinase-3. *The Journal of Biological Chemistry*, *283*(32), 21934–21944. https://doi.org/10.1074/jbc.M802481200

Blumcke, I., Thom, M., Aronica, E., Armstrong, D. D., Bartolomei, F., Bernasconi, A., Bernasconi, N., Bien, C. G., Cendes, F., Coras, R., Cross, J. H., Jacques, T. S., Kahane, P., Mathern, G. W., Miyata, H., Moshé, S. L., Oz, B., Özkara, Ç., Perucca, E., ... Spreafico, R. (2013). International consensus classification of hippocampal sclerosis in temporal lobe epilepsy: A task force report from the ILAE commission on diagnostic methods. *Epilepsia*, *54*(7), 1315–1329. https://doi.org/10.1111/epi.12220

Bowers, M. B., Jr., & Heninger, G. R. (1977). Lithium: Clinical effects and cerebrospinal fluid acid monoamine metabolites. *Communications in Psychopharmacology*, *1*(2), 135–145. http://www.ncbi.nlm.nih.gov/pubmed/603996

Bronstein, R., Torres, L., Nissen, J. C., & Tsirka, S. E. (2013). Culturing microglia from the neonatal and adult central nervous system. *Journal of Visualized Experiments*, *78*, 50647. https://doi.org/10.3791/50647

Cao, Q., Karthikeyan, A., Dheen, S. T., Kaur, C., & Ling, E. A. (2017). Production of proinflammatory mediators in activated microglia is synergistically regulated by Notch-1, glycogen synthase kinase (GSK-3beta) and NF-kappaB/p65 signalling. *PLoS One*, *12*(10), e0186764. https://doi.org/10.1371/journal.pone.0186764

Carrillo-Jimenez, A., Deniz, O., Niklison-Chirou, M. V., Ruiz, R., Bezerra-Salomao, K., Stratoulias, V., Amouroux, R., Yip, P. K., Vilalta, A., Cheray, M., & Scott-Egerton, A. M. (2019). TET2 regulates the neuroinflammatory response in microglia. *Cell Reports*, *29*(3), 697–713 e698. https://doi.org/10.1016/j.celrep.2019.09.013

Chalecka-Franaszek, E., & Chuang, D. M. (1999). Lithium activates the serine/threonine kinase Akt-1 and suppresses glutamate-induced inhibition of Akt-1 activity in neurons. *Proceedings of the National Academy of Sciences of the United States of America*, *96*(15), 8745–8750. https://doi.org/10.1073/pnas.96.15.8745

Cipriani, A., Hawton, K., Stockton, S., & Geddes, J. R. (2013). Lithium in the prevention of suicide in mood disorders: Updated systematic review and meta-analysis. *BMJ*, *346*, f3646. https://doi.org/10.1136/bmj.f3646

Coghlan, M. P., Culbert, A. A., Cross, D. A., Corcoran, S. L., Yates, J. W., Pearce, N. J., Rausch, O. L., Murphy, G. J., Carter, P. S., Cox, L. R., Mills, D., & Holder, J. C. (2000). Selective small molecule inhibitors of glycogen synthase kinase-3 modulate glycogen metabolism and gene transcription. *Chemistry & Biology*, 7(10), 793–803. https://doi.org/10.1016/s1074-5521(00)00025-9

Colonna, M., & Butovsky, O. (2017). Microglia function in the central nervous system during health and neurodegeneration. *Annual Review of Immunology*, 35, 441–468. https://doi.org/10.1146/annurev-immunol-051116-052358

Darnell, J. E., Jr., Kerr, I. M., & Stark, G. R. (1994). Jak-STAT pathways and transcriptional activation in response to IFNs and other extracellular signaling proteins. *Science*, 264(5164), 1415–1421. https://doi.org/10.1126/science.8197455

Davenport, C. M., Sevastou, I. G., Hooper, C., & Pocock, J. M. (2010). Inhibiting p53 pathways in microglia attenuates microglial-evoked neurotoxicity following exposure to Alzheimer peptides. *Journal of Neurochemistry*, 112(2), 552–563. https://doi.org/10.1111/j.1471-4159.2009.06485.x

Dong, H., Zhang, X., Dai, X., Lu, S., Gui, B., Jin, W., Zhang, S., Zhang, S., & Qian, Y. (2014). Lithium ameliorates lipopolysaccharide-induced microglial activation via inhibition of toll-like receptor 4 expression by activating the PI3K/Akt/FoxO1 pathway. *Journal of Neuroinflammation*, 11, 140. https://doi.org/10.1186/s12974-014-0140-4

Eisenberg, E., & Levanon, E. Y. (2013). Human housekeeping genes, revisited. *Trends in Genetics*, 29(10), 569–574. https://doi.org/10.1016/j.tig.2013.05.010

Feinstein, D. L. (1998). Potentiation of astroglial nitric oxide synthase type-2 expression by lithium chloride. *Journal of Neurochemistry*, 71(2), 883–886. https://doi.org/10.1046/j.1471-4159.1998.71020883.x

Frugier, T., Morganti-Kossmann, M. C., O'Reilly, D., & McLean, C. A. (2010). In situ detection of inflammatory mediators in post mortem human brain tissue after traumatic injury. *Journal of Neurotrauma*, 27(3), 497–507. https://doi.org/10.1089/neu.2009.1120

Fyro, B., Petterson, U., & Sedvall, G. (1975). The effect of lithium treatment on manic symptoms and levels of monoamine metabolites in cerebrospinal fluid of manic depressive patients. *Psychopharmacologia*, 44(1), 99–103. https://doi.org/10.1007/bf00421192

Geddes, J. R., Burgess, S., Hawton, K., Jamison, K., & Goodwin, G. M. (2004). Long-term lithium therapy for bipolar disorder: Systematic review and meta-analysis of randomized controlled trials. *The American Journal of Psychiatry*, 161(2), 217–222. https://doi.org/10.1176/appi.ajp.161.2.217

Huang, W. C., Lin, Y. S., Wang, C. Y., Tsai, C. C., Tseng, H. C., Chen, C. L., Lu, P. J., Chen, P. S., Qian, L., Hong, J. S., & Lin, C. F. (2009). Glycogen synthase kinase-3 negatively regulates anti-inflammatory interleukin-10 for lipopolysaccharide-induced iNOS/NO biosynthesis and RANTES production in microglial cells. *Immunology*, 128(1 Suppl), 275–286. https://doi.org/10.1111/j.1365-2567.2008.02959.x

Jeon, S. W., & Kim, Y. K. (2016). Neuroinflammation and cytokine abnormality in major depression: Cause or consequence in that illness? *World J Psychiatry*, 6(3), 283–293. https://doi.org/10.5498/wjp.v6.i3.283

Jope, R. S., & Johnson, G. V. (2004). The glamour and gloom of glycogen synthase kinase-3. *Trends in Biochemical Sciences*, 29(2), 95–102. https://doi.org/10.1016/j.tibs.2003.12.004

Klein, P. S., & Melton, D. A. (1996). A molecular mechanism for the effect of lithium on development. *Proceedings of the National Academy of Sciences of the United States of America*, 93(16), 8455–8459. https://doi.org/10.1073/pnas.93.16.8455

Komoroski, R. A., Pearce, J. M., & Newton, J. E. (1997). The distribution of lithium in rat brain and muscle in vivo by 7Li NMR imaging. *Magnetic Resonance in Medicine*, 38(2), 275–278. https://doi.org/10.1002/mrm.1910380217

Kopschina Feltes, P., Doorduin, J., Klein, H. C., Juarez-Orozco, L. E., Dierckx, R. A., Moriguchi-Jeckel, C. M., & de Vries, E. F. (2017). Anti-inflammatory treatment for major depressive disorder: Implications for patients with an elevated immune profile and non-responders to standard antidepressant therapy. *Journal of Psychopharmacology*, 31(9), 1149–1165. https://doi.org/10.1177/0269881117711708

Malhi, G. S., Gessler, D., & Outhred, T. (2017). The use of lithium for the treatment of bipolar disorder: Recommendations from clinical practice guidelines. *Journal of Affective Disorders*, 217, 266–280. https://doi.org/10.1016/j.jad.2017.03.052

Mann, J. J., Arango, V., Marzuk, P. M., Theccanat, S., & Reis, D. J. (1989). Evidence for the 5-HT hypothesis of suicide. A review of post-mortem studies. *The British Journal of Psychiatry*, S8, 7–14. http://www.ncbi.nlm.nih.gov/pubmed/2692642

McKim, D. B., Weber, M. D., Niraula, A., Sawicki, C. M., Liu, X., Jarrett, B. L., Ramirez-Chan, K., Wang, Y., Roeth, R. M., Sucaldito, A. D., Sobol, C. G., Quan, N., Sheridan, J. F., & Godbout, J. P. (2018). Microglial recruitment of IL-1beta-producing monocytes to brain endothelium causes stress-induced anxiety. *Molecular Psychiatry*, 23(6), 1421–1431. https://doi.org/10.1038/mp.2017.64

Muller-Oerlinghausen, B. (1985). Lithium long-term treatment—does it act via serotonin? *Pharmacopsychiatry*, 18(2), 214–217. https://doi.org/10.1055/s-2007-1017367

Nahman, S., Belmaker, R. H., & Azab, A. N. (2012). Effects of lithium on lipopolysaccharide-induced inflammation in rat primary glia cells. *Innate Immunity*, 18(3), 447–458. https://doi.org/10.1177/1753425911421512

Nelson, E. A., Walker, S. R., Kepich, A., Gashin, L. B., Hideshima, T., Ikeda, H., Chauhan, D., Anderson, K. C., & Frank, D. A. (2008). Nifuroxazide inhibits survival of multiple myeloma cells by directly inhibiting STAT3. *Blood*, 112(13), 5095–5102. https://doi.org/10.1182/blood-2007-12-129718

Nguyen, H. M., Grossinger, E. M., Horiuchi, M., Davis, K. W., Jin, L. W., Maezawa, I., & Wulff, H. (2017). Differential Kv1.3, KCa3.1, and Kir2.1 expression in "classically" and "alternatively" activated microglia. *Glia*, 65(1), 106–121. https://doi.org/10.1002/glia.23078

Nie, X., Kitaoka, S., Tanaka, K., Segi-Nishida, E., Imoto, Y., Ogawa, A., Nakano, F., Tomohiro, A., Nakayama, K., Taniguchi, M., Mimori-Kiyosue, Y., Kakizuka, A., Narumiya, S., & Furuyashiki, T. (2018). The innate immune receptors TLR2/4 mediate repeated social defeat stress-induced social avoidance through prefrontal microglial activation. *Neuron*, 99(3), 464–479. https://doi.org/10.1016/j.neuron.2018.06.035

Perez-Cruet, J., Tagliamonte, A., Tagliamonte, P., & Gessa, G. L. (1971). Stimulation of serotonin synthesis by lithium. *The Journal of Pharmacology and Experimental Therapeutics*, 178(2), 325–330. https://www.ncbi.nlm.nih.gov/pubmed/5570457

Prakash, S., Adroja, B., & Parekh, H. (2017). Serotonin syndrome in patients with headache disorders. *BML Case Reports*, 2017. bcr-2017-221383. https://doi.org/10.1136/bcr-2017-221383

Roy, A., De Jong, J., & Linnoila, M. (1989). Cerebrospinal fluid monoamine metabolites and suicidal behavior in depressed patients. A 5-year follow-up study. *Archives of General Psychiatry*, 46(7), 609–612. https://doi.org/10.1001/archpsyc.1989.01810070035005

Rustenhoven, J., Park, T. I., Schweder, P., Scotter, J., Correia, J., Smith, A. M., Gibbons, H. M., Oldfield, R. L., Bergin, P. S., Mee, E. W., Faull, R. L. M., Curtis, M. A., Scott Graham, E., & Dragunow, M. (2016). Isolation of highly enriched primary human microglia for functional studies. *Scientific Reports*, 6, 19371. https://doi.org/10.1038/srep19371

Schmidt, S. V., & Schultze, J. L. (2014). New insights into IDO biology in bacterial and viral infections. *Frontiers in Immunology*, 5, 384. https://doi.org/10.3389/fimmu.2014.00384

Seok, J., Warren, H. S., Cuenca, A. G., Mindrinos, M. N., Baker, H. V., Xu, W., Richards, D. R., McDonald-Smith, G. P., Gao, H., Hennessy, L., & Finnerty, C. C. (2013). Genomic responses in mouse models poorly mimic human inflammatory diseases. *Proceedings of the National Academy of Sciences of the United States of America*, 110(9), 3507–3512. https://doi.org/10.1073/pnas.1222878110

Smith, F. E., Thelwall, P. E., Necus, J., Flowers, C. J., Blamire, A. M., & Cousins, D. A. (2018). 3D (7)li magnetic resonance imaging of brain lithium distribution in bipolar disorder. *Molecular Psychiatry*, 23(11), 2184–2191. https://doi.org/10.1038/s41380-018-0016-6

Smith, K. A., & Cipriani, A. (2017). Lithium and suicide in mood disorders: Updated meta-review of the scientific literature. *Bipolar Disorders*, 19(7), 575–586. https://doi.org/10.1111/bdi.12543

Sobanski, T., Bagli, M., Laux, G., & Rao, M. L. (1997). Serotonin syndrome after lithium add-on medication to paroxetine. *Pharmacopsychiatry*, 30(3), 106–107. https://doi.org/10.1055/s-2007-979491

Stambolic, V., Ruel, L., & Woodgett, J. R. (1996). Lithium inhibits glycogen synthase kinase-3 activity and mimics wingless signalling in intact cells. *Current Biology*, 6(12), 1664–1668. https://doi.org/10.1016/s0960-9822(02)70790-2

Sullivan, G. M., Oquendo, M. A., Milak, M., Miller, J. M., Burke, A., Ogden, R. T., Parsey, R. V., & Mann, J. J. (2015). Positron emission tomography quantification of serotonin(1A) receptor binding in suicide attempters with major depressive disorder. *JAMA Psychiatry*, 72(2), 169–178. https://doi.org/10.1001/jamapsychiatry.2014.2406

Sutherland, C., Leighton, I. A., & Cohen, P. (1993). Inactivation of glycogen synthase kinase-3 beta by phosphorylation: New kinase connections in insulin and growth-factor signalling. *The Biochemical Journal*, 296(Pt 1), 15–19. https://doi.org/10.1042/bj2960015

Tam, W. Y., & Ma, C. H. (2014). Bipolar/rod-shaped microglia are proliferating microglia with distinct M1/M2 phenotypes. *Scientific Reports*, 4, 7279. https://doi.org/10.1038/srep07279

Tiihonen, J. (2017). Use of lithium in patients with unipolar depression—Author's reply. *Lancet Psychiatry*, 4(9), 663. https://doi.org/10.1016/S2215-0366(17)30319-X

Torres-Platas, S. G., Cruceanu, C., Chen, G. G., Turecki, G., & Mechawar, N. (2014). Evidence for increased microglial priming and macrophage recruitment in the dorsal anterior cingulate white matter of depressed suicides. *Brain, Behavior, and Immunity*, 42, 50–59. https://doi.org/10.1016/j.bbi.2014.05.007

Tsai, C. C., Kai, J. I., Huang, W. C., Wang, C. Y., Wang, Y., Chen, C. L., Fang, Y. T., Lin, Y. S., Anderson, R., Chen, S. H., Tsao, C. W., & Lin, C. F. (2009). Glycogen synthase kinase-3beta facilitates IFN-gamma-induced STAT1 activation by regulating Src homology-2 domain-containing phosphatase 2. *Journal of Immunology*, 183(2), 856–864. https://doi.org/10.4049/jimmunol.0804033

Uhlemann, R., Gertz, K., Boehmerle, W., Schwarz, T., Nolte, C., Freyer, D., Kettenmann, H., Endres, M., & Kronenberg, G. (2016). Actin dynamics shape microglia effector functions. *Brain Structure & Function*, 221(5), 2717–2734. https://doi.org/10.1007/s00429-015-1067-y

van Baren, N., & van den Eynde, B. J. (2015). Tryptophan-degrading enzymes in tumoral immune resistance. *Frontiers in Immunology*, 6, 34. https://doi.org/10.3389/fimmu.2015.00034

Ward, M. E., Musa, M. N., & Bailey, L. (1994). Clinical pharmacokinetics of lithium. *Journal of Clinical Pharmacology*, 34(4), 280–285. https://doi.org/10.1002/j.1552-4604.1994.tb01994.x

Woodgett, J. R. (1990). Molecular cloning and expression of glycogen synthase kinase-3/factor a. *The EMBO Journal*, 9(8), 2431–2438. http://www.ncbi.nlm.nih.gov/pubmed/2164470

Yirmiya, R., Rimmerman, N., & Reshef, R. (2015). Depression as a microglial disease. *Trends in Neurosciences*, 38(10), 637–658. https://doi.org/10.1016/j.tins.2015.08.001

Yuskaitis, C. J., & Jope, R. S. (2009). Glycogen synthase kinase-3 regulates microglial migration, inflammation, and inflammation-induced neurotoxicity. *Cellular Signalling*, 21(2), 264–273. https://doi.org/10.1016/j.cellsig.2008.10.014

Zheng, H., Jia, L., Liu, C. C., Rong, Z., Zhong, L., Yang, L., Chen, X. F., Fryer, J. D., Wang, X., Zhang, Y. W., Xu, H., & Bu, G. (2017). TREM2 promotes microglial survival by activating Wnt/beta-catenin pathway. *The Journal of Neuroscience*, 37(7), 1772–1784. https://doi.org/10.1523/JNEUROSCI.2459-16.2017

SUPPORTING INFORMATION

Additional supporting information may be found in the online version of the article at the publisher's website.